Optics Letters

Direct regenerative amplification of femtosecond pulses to the multimillijoule level

Moritz Ueffing,[1,*] Robert Lange,[1] Tobias Pleyer,[1] Vladimir Pervak,[1] Thomas Metzger,[2] Dirk Sutter,[3] Zsuzsanna Major,[1,4] Thomas Nubbemeyer,[1] and Ferenc Krausz[1,4]

[1]Ludwig-Maximilians-Universität München, Am Coulombwall 1, 85748 Garching, Germany
[2]TRUMPF Scientific Lasers GmbH + Co. KG, Feringastr. 10a, 85774 München-Unterföhring, Germany
[3]TRUMPF Laser GmbH, Aichhalder Str. 39, 78713 Schramberg, Germany
[4]Max-Planck-Institut für Quantenoptik, Hans-Kopfermann-Str. 1, 85748 Garching, Germany
*Corresponding author: moritz.ueffing@mpq.mpg.de

Received 14 July 2016; accepted 18 July 2016; posted 20 July 2016 (Doc. ID 270594); published 10 August 2016

We present a compact femtosecond nonlinear Yb:YAG thin-disk regenerative amplifier delivering pulses carried at a wavelength of 1030 nm with an average power of >200 W at a repetition rate of 100 kHz and an energy noise value of 0.46% (rms) in a beam with a propagation factor of $M^2 < 1.4$. The amplifier is seeded with bandwidth-limited subpicosecond pulses without temporal stretching. We give estimates for the nonlinear parameters influencing the system and show that chirped mirrors compress the 2 mJ pulses to a near-bandwidth-limited duration of 210 fs.

OCIS codes: (140.3615) Lasers, ytterbium; (140.4480) Optical amplifiers; (140.3480) Lasers, diode-pumped; (320.7090) Ultrafast lasers; (320.5520) Pulse compression.

http://dx.doi.org/10.1364/OL.41.003840

Femtosecond sources for attosecond science have so far been based on Ti:sapphire (Ti:Sa) laser systems that provide millijoule-scale pulses with spectral bandwidths supporting pulse durations of typically less than 5 fs [1–3], building well-developed sources for attosecond science [4]. Ti:Sa laser systems, however, are limited to average power levels of ∼10 W [5] by thermal problems. High-repetition-rate driving lasers would benefit attosecond metrology and spectroscopy in many applications, including coincidence measurements and spectroscopy of low-cross-section systems [6,7].

Overcoming the average power limitation of Ti:Sa systems in multimillijoule (multi-mJ) femtosecond pulse generation is challenging and constitutes a hot topic in current laser development. Established gain media supporting 0.1–1 kW output power, such as Yb-doped materials, have much narrower gain bands [8]. Nevertheless, these media have been the basis for several improvements in energy scaling of mode-locked oscillators [9–11], fiber lasers [12], and optical parametric chirped-pulse amplifiers (OPCPAs) [13–15].

Ytterbium laser amplifiers have so far relied on chirped-pulse amplification (CPA) to deliver multi-mJ pulse energies in order to avoid damage or nonlinear effects during the amplification process. CPA systems, such as fiber laser amplifiers [12], Yb:YAG thin-disk amplifiers [16–18], and Innoslab amplifiers [19], routinely deliver multi-mJ pulse energies at repetition rates from a few kilohertz (kHz) to several hundred kHz. Additionally, cryogenic Yb:YAG amplifiers have proven to deliver multi-mJ pulses [20]. These architectures provide pulse durations of 200 fs (fiber) or <0.4–3.6 ps (thin-disk, Innoslab, and cryogenic systems) and are rapidly proliferating as drivers of pulse compressors and OPCPA systems. Implementing CPA in Yb-doped fiber amplifiers, however, requires large amounts of group delay dispersion (GDD) and, hence, expensive, large-aperture gratings for stretching and recompression [21].

The millijoule-scale pulse energy of high repetition rate systems suggests that avoiding CPA to reduce both the complexity and the cost of the amplifier is feasible using an amplifier with reduced nonlinearity [22–24]. A pulse duration considerably shorter than 1 ps is beneficial to allow for both direct compression of the laser output toward the single cycle regime and efficiently pumping femtosecond optical parametric amplifiers.

In amplifiers based on direct amplification of short pulses (∼1 ps), nonlinear optical effects even prove beneficial [16,25–27]. Self-phase modulation (SPM) in these systems leads to an increase of the spectral bandwidth of the pulses during amplification. Consequently, gain narrowing can be overcome. Systems based on this approach have been demonstrated with a pulse energy of up to 360 μJ at 100 kHz repetition rate with pulse duration of <300 fs (Yb:YAG) [28].

Here we report CPA-free short pulse generation in an Yb:YAG thin-disk regenerative amplifier by exploiting SPM-induced spectral broadening during the amplification process. We have obtained 2.0 mJ pulses with 210 fs (FWHM) pulse duration at 100 kHz repetition rate. The resultant peak power of 7.3 GW fills the gap between high-power oscillators and CPA systems.

The front end for the regenerative amplifier [see Fig. 1(a)] is based on a Menlo Orange Yb-fiber oscillator emitting 100 mW at 100 MHz repetition rate. A rubidium titanyl phosphate (RTP) pulse picker reduces the repetition rate to 100 kHz. The oscillator delivers stretched pulses of ∼2 ps duration,

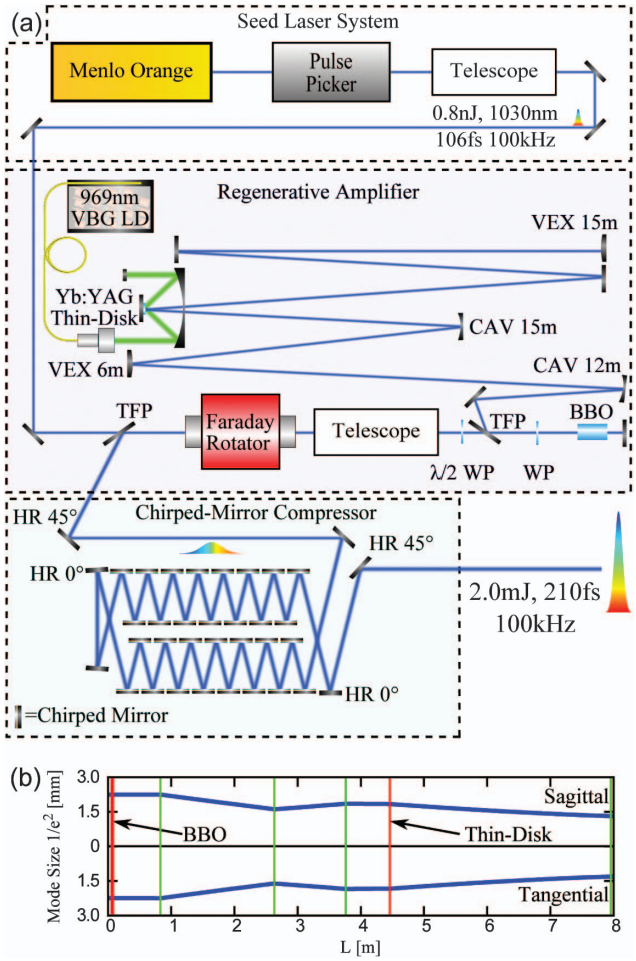

Fig. 1. (a) Schematic layout of the amplifier. The seed laser system is based on a 100 MHz, 100 mW Menlo Systems Yb-fiber laser. The regenerative amplifier consists of an isolator stage composed of a thin-film polarizer (TFP), a Faraday rotator (FR), and a $\lambda/2$-wave plate (WP). Directly following the FR a second telescope reduces the beam to match the cavity mode size at the entry of the cavity. The optical switch inside the cavity contains a β – BaB_2O_4 (BBO) crystal and a wave plate. The compressor consists of 30 chirped mirrors. (b) Calculated eigenmode of the resonator. The vertical lines represent the positions of the curved mirrors and the transmissive optical elements.

which are compressed with a compact grating pair to allow seeding the regenerative amplifier with 106 fs near-bandwidth-limited pulses of a spectral bandwidth of 30 nm (FWHM) and a pulse energy 0.8 nJ.

An isolator consisting of a thin-film-polarizer (TFP), a $\lambda/2$-wave plate and Faraday rotator separates the input and output pulses. The Faraday rotator contains a 20 mm thick terbium gallium garnet (TGG) crystal with an aperture of 20 mm, allowing transmission of a beam with a diameter of ~9 mm ($1/e^2$) to minimize nonlinearities introduced by the TGG crystal after amplification. A telescope behind the rotator reduces the beam diameter to 4.5 mm ($1/e^2$), matching the diameter to the resonator eigenmode.

The linear resonator of the regenerative amplifier [Fig. 1(b)] includes a β – BaB_2O_4 (BBO) crystal with 10 mm × 10 mm clear aperture (12 mm × 12 mm total area) and a length of 20 mm. It is switched with a high-voltage, high-average-power driver provided by Bergmann Messgeräte Entwicklung KG. The voltage applied to the crystal is ~13.5 kV at 100 kHz repetition rate. The amplification time within the cavity is set to 5.795 µs, leading to 110 full round trips in the resonator.

The pulse is amplified by a 0.1 mm Yb:YAG thin-disk provided by TRUMPF Laser GmbH, having a diameter of 9 mm and a radius of curvature (RoC) of ≈20 m. The thin-disk is pumped into its zero-phonon line using a 969 nm pump diode module (TRUMPF Laser GmbH) and a pump spot diameter of 4.0–4.5 mm ($1/e^2$). The amplifying resonator is designed to match both the aperture of the BBO crystal and the pump spot diameter of the thin disk.

After amplification, a compressor based on 30 chirped mirrors introducing a GDD of –2000 fs^2 each removes the chirp introduced by SPM of the output pulses. The compressor setup covers a total area of 45 cm × 60 cm.

680 W of pump power leads to an output energy of 2.1 mJ at 100 kHz repetition rate. This amounts to an overall optical-to-optical efficiency of 31%. The slope efficiency of the system is 38%. The moderate efficiency of the amplifier is considered to be connected to the emerging nonlinear loss channels [29–31].

Figure 2 shows the output spectra for the different amplification levels controlled by the pump power while keeping the round trips inside the cavity constant. It can be seen that, for pulse energies lower than 100 µJ, only spectral components significantly overlapping with the peak of the Yb:YAG emission cross section [8] are amplified, leading to the well-known gain narrowing effect. This results in significant spectral narrowing of the pulse and lengthening of the pulse to ~1 ps. With increasing pulse energy, nonlinear effects, primarily introduced by the BBO crystal, become important and SPM broadens the spectrum to reach >10 nm at 2 mJ pulse energy. The output spectrum calculated with our 1D-split-step model shows good agreement with the measured spectrum (Fig. 2). The effective nonlinear refractive index used in this model amounts to $n_{2_{\text{eff}}} = 0.24 \cdot n_{2_{\text{BBO}}}$, where $n_{2_{\text{BBO}}} = 5.6 \cdot 10^{-20}$ m^2/W [32]. The calculated B-integral amounts to 7.2 rad.

Self-focusing constitutes the second nonlinear influence on the system. At gigawatt peak power levels, self-focusing caused by the BBO crystal gradually alters the wavefront during the amplification process. In a first approximation, the nonlinear lens introduces an additional focusing element, the refractive power of which scales linearly with the peak power of the pulse [31]:

$$D_{\text{NL}} \approx \frac{4n_{2_{\text{eff}}}L}{\pi w^4} \cdot P_{\text{peak}} = \frac{4n_{2_{\text{eff}}}L}{\pi w^4} \cdot \sqrt{\frac{2}{\pi}}\frac{E}{\tau} = c_{\text{NL}} \cdot E, \quad (1)$$

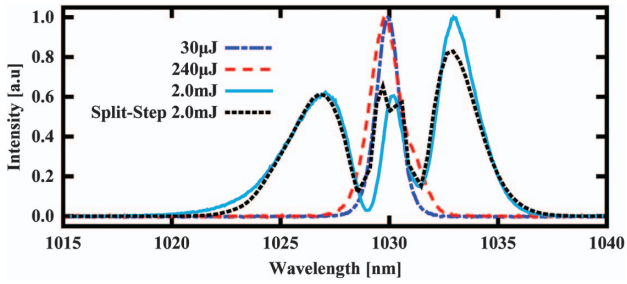

Fig. 2. Simulated and measured output spectra for different pulse energies. Above the threshold of ~100 µJ, SPM broadens the spectrum of the laser pulse.

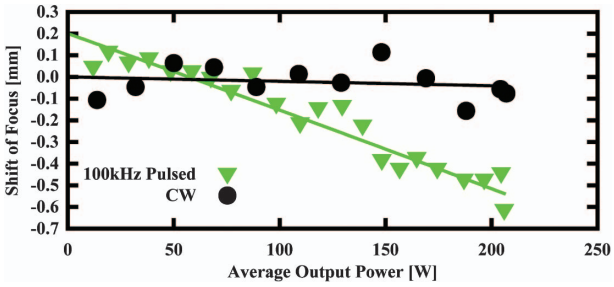

Fig. 3. Measured shift of the focal position in CW and pulsed mode. The green solid line shows the fitted function. The black line shows a linear fit to the CW data points.

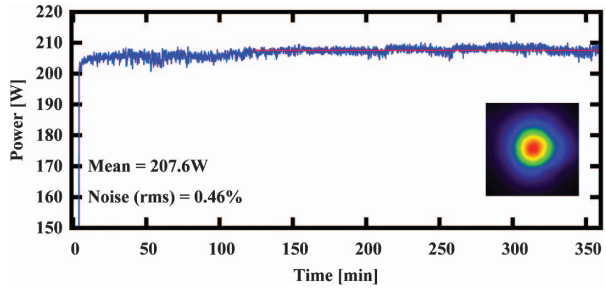

Fig. 5. Measured long-term stability of the system. The system was started in a cold state. After a 2 h warming-up phase, the system stayed at 207 W with a noise value of 0.46% (rms). The inset shows the beam profile of the output beam.

where P_{peak} is the peak power of the pulse, w is the mode radius (4.5/2 mm), L is the length of the nonlinear medium (BBO crystal, 20 mm), E is the pulse energy, τ is the pulse duration (1.4 ps), and $n_{2_{eff}}$ represents an effective nonlinear refractive index. To get an estimate for D_{NL}, the position of the focus of the output laser beam was measured both in CW and in 100 kHz pulsed mode. Figure 3 depicts this change for different output powers where the output power in CW is adjusted to reach the same output power as in pulsed mode at 680 W pump power. By comparing the behavior of the laser operating in CW and at 100 kHz, it is possible to estimate the value of the nonlinear lens according to Eq. (1). By fitting the ABCD transition matrix, we obtain $n_{2_{eff}} = 0.15 \cdot n_{2_{BBO}}$ or $c_{NL} = 4.6$ dpt/J. In comparing this result with the 1D-split-step model describing the nonlinear behavior in the temporal domain, we find a consistent reduction of the nonlinear refractive index $n_{2_{BBO}}$. The refractive power calculated from this estimation is lower than 0.01 diopter (dpt) at 2 mJ pulse energy.

To guarantee a stable amplification process it is necessary to match the laser mode for every round trip to the pump spot on the thin disk. The resonator design shows low sensitivity of the mode diameter at the thin disk to the changing nonlinear lens for the parameter range estimated from the fitted value, as can be seen from the calculations of the mode size in the cavity for different refractive powers of the nonlinear focusing element shown in Fig. 4. This ensures a good overlap between the pump beam diameter and the beam inside the cavity over a wide pulse energy range.

Importantly, the resonator mode has no tightly focused waist, allowing for amplification in air. Small beam diameters or foci would otherwise limit the pulse energy to much lower values than those that are presented here. To minimize the contribution of air, the resonator eigenmode has a minimum beam diameter of more than 2.6 mm ($1/e^2$) [Fig. 1(b)].

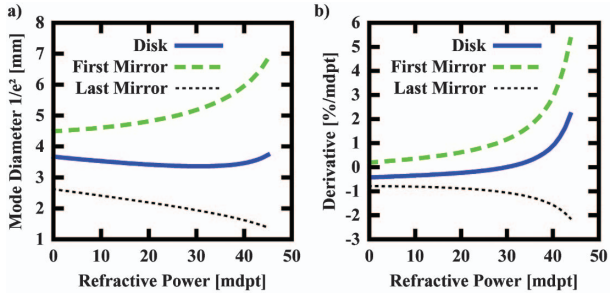

Fig. 4. (a) ABCD matrix calculation showing the eigenmode size change at the two end mirrors and the disk with respect to a focusing element at the position of the BBO crystal. (b) Relative change of the functions shown in (a).

Figure 5 depicts the output power of the amplifier (measured with an Ophir FL500A-BB-65 power head). The measurement shows 6 h of operation starting from a cold system. After a time of approximately 2 h, the system stays at the desired 207 W output power with less than 0.5% rms fluctuation. The pulse-to-pulse stability of the laser was measured by recording 5000 subsequent pulses with a photodiode and shows an upper bound of the rms pulse-to-pulse noise of 0.43%.

The output beam quality is close to the diffraction limit with an $M^2 < 1.4$. The beam quality was measured using a commercial Spiricon M^2 – 200 s taking the 4σ beam diameter.

The nonlinear spectral phase and the intracavity GDD (dominated by the BBO crystal) introduce a positive chirp to the 2.1 mJ output pulses. This results in an output pulse duration of 1.4 ps (FWHM). A compressor consisting of 30 chirped mirrors compresses the output pulses. Each mirror has a GDD of -2000 fs^2, leading to $\sim 6 \cdot 10^4$ fs^2 in total. The characterization of the electric field using second-harmonic frequency resolved optical gating (SH-FROG) shows that the compressor almost perfectly removes the chirp carried by the output pulses (see Fig. 6). The resulting pulse duration of 210 fs (FWHM) is close to the Fourier limit [205 fs (FWHM)] and shows only minor

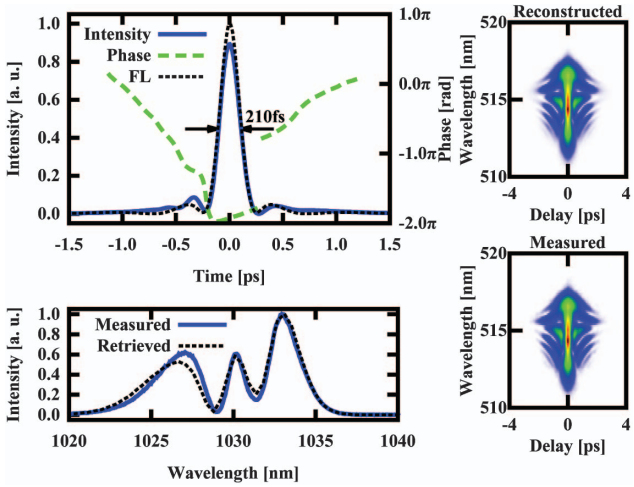

Fig. 6. SH-FROG measurement of the compressed output pulses (FROG error: $3.166 \cdot 10^{-3}$). The pulses are very close to the Fourier limit (FL), showing an excellent temporal profile.

satellites. The retrieved spectrum of the SH-FROG measurement is in excellent agreement with the measured spectrum of the pulse at 2 mJ (see Fig. 2), indicating good reconstruction of the electric field. The ratio of the peak power between the Fourier limit and the compressed pulse is 89%. The efficiency over the whole 35 mirrors in the compressor setup (chirped mirrors + folding mirrors) amounts to 97%, leading to 2.0 mJ pulse energy and 7.3 GW peak power.

Our experiments show that the system can be operated at variable repetition rates from a few kilohertz to 100 kHz. Up to this level we did not observe restrictions in average power scaling. Thus, the system holds promise to be scalable to higher repetition rates. Currently, repetition rate scaling of the system is considered to be linked to the maximum achievable repetition rate as provided by the high voltage Pockels cell driver.

In conclusion, we have demonstrated a powerful CPA-free nonlinear Yb:YAG thin-disk regenerative amplifier. The system is capable of running for hours at stable output power of >200 W at 100 kHz repetition rate. The gain-bandwidth limitation is overcome by SPM inside the resonator of the regenerative amplifier. Although the laser runs in a strongly nonlinear regime, M^2 of the output beam was measured to be <1.4, indicating an efficient spatial filtering in the resonator. Furthermore, we have proven that the 2.1 mJ output pulses can be compressed to be nearly Fourier limited. The 210 fs pulse duration (FWHM) in combination with the 97% efficiency of the chirped mirror compressor results in a pulse energy of 2.0 mJ and 7.3 GW peak power after compression. The measurements clearly show that the system is stable enough for further usage as a driving laser for nonlinear optics. The laser pulse duration is ideal for further external nonlinear compression stages in cascaded second-order nonlinear processes [33,34] or noble-gas-filled hollow core fibers [35]. External nonlinear compression stages may render the described amplifier an ideal source of high-repetition-rate few-cycle laser pulses for attosecond pulse generation and spectroscopy.

Funding. Munich-Centre for Advanced Photonics (MAP); Center for Advanced Laser Applications (CALA).

Acknowledgment. We thank Martin Gorjan, Hanieh Fattahi, Jonathan Brons, Florian Saran, and Helena G. Barros for their support.

REFERENCES

1. M. Nisoli, S. De Silvestri, and O. Svelto, Appl. Phys. Lett. **68**, 2793 (1996).
2. B. Schenkel, J. Biegert, U. Keller, C. Vozzi, M. Nisoli, G. Sansone, S. Stagira, S. D. Silvestri, and O. Svelto, Opt. Lett. **28**, 1987 (2003).
3. A. L. Cavalieri, E. Goulielmakis, B. Horvath, W. Helml, M. Schultze, M. Fieß, V. Pervak, L. Veisz, V. S. Yakovlev, M. Uiberacker, A. Apolonski, F. Krausz, and R. Kienberger, New J. Phys. **9**, 242 (2007).
4. F. Krausz and M. Ivanov, Rev. Mod. Phys. **81**, 163 (2009).
5. I. Matsushima, H. Yashiro, and T. Tomie, Opt. Lett. **31**, 2066 (2006).
6. S. R. Leone, C. W. McCurdy, J. Burgdorfer, L. S. Cederbaum, Z. Chang, N. Dudovich, J. Feist, C. H. Greene, M. Ivanov, R. Kienberger, U. Keller, M. F. Kling, Z.-H. Loh, T. Pfeifer, A. N. Pfeiffer, R. Santra, K. Schafer, A. Stolow, U. Thumm, and M. J. J. Vrakking, Nat. Photonics **8**, 162 (2014).
7. G. Sansone, F. Kelkensberg, F. Morales, J. Perez-Torres, F. Martín, and M. Vrakking, IEEE J. Sel. Top. Quantum Electron. **18**, 520 (2012).
8. J. Koerner, C. Vorholt, H. Liebetrau, M. Kahle, D. Kloepfel, R. Seifert, J. Hein, and M. C. Kaluza, J. Opt. Soc. Am. B **29**, 2493 (2012).
9. J. Brons, V. Pervak, E. Fedulova, D. Bauer, D. Sutter, V. Kalashnikov, A. Apolonskiy, O. Pronin, and F. Krausz, Opt. Lett. **39**, 6442 (2014).
10. D. Bauer, I. Zawischa, D. H. Sutter, A. Killi, and T. Dekorsy, Opt. Express **20**, 9698 (2012).
11. C. J. Saraceno, F. Emaury, O. H. Heckl, C. R. E. Baer, M. Hoffmann, C. Schriber, M. Golling, T. Südmeyer, and U. Keller, Opt. Express **20**, 23535 (2012).
12. A. Klenke, S. Hädrich, T. Eidam, J. Rothhardt, M. Kienel, S. Demmler, T. Gottschall, J. Limpert, and A. Tünnermann, Opt. Lett. **39**, 6875 (2014).
13. H. Fattahi, H. G. Barros, M. Gorjan, T. Nubbemeyer, B. Alsaif, C. Y. Teisset, M. Schultze, S. Prinz, M. Haefner, M. Ueffing, A. Alismail, L. Vámos, A. Schwarz, O. Pronin, J. Brons, X. T. Geng, G. Arisholm, M. Ciappina, V. S. Yakovlev, D.-E. Kim, A. M. Azzeer, N. Karpowicz, D. Sutter, Z. Major, T. Metzger, and F. Krausz, Optica **1**, 45 (2014).
14. M. Puppin, Y. Deng, O. Prochnow, J. Ahrens, T. Binhammer, U. Morgner, M. Krenz, M. Wolf, and R. Ernstorfer, Opt. Express **23**, 1491 (2015).
15. S. Prinz, M. Haefner, C. Y. Teisset, R. Bessing, K. Michel, Y. Lee, X. T. Geng, S. Kim, D. E. Kim, T. Metzger, and M. Schultze, Opt. Express **23**, 1388 (2015).
16. O. H. Heckl, J. Kleinbauer, D. Bauer, S. Weiler, T. Metzger, and D. H. Sutter, *Ultrashort Pulse Laser Technology* (Springer, 2016), pp. 93–115.
17. S. Klingebiel, M. Schultze, C. Y. Teisset, R. Bessing, M. Häfner, S. Prinz, M. Gorjan, D. Sutter, K. Michel, H. G. Barros, Z. Major, F. Krausz, and T. Metzger, in *European Conference on Lasers and Electro-Optics-European Quantum Electronics Conference* (Optical Society of America, 2015), paper CA_10_1.
18. W. Schneider, A. Ryabov, C. Lombosi, T. Metzger, Z. Major, J. A. Fülöp, and P. Baum, Opt. Lett. **39**, 6604 (2014).
19. P. Russbueldt, D. Hoffmann, M. Hofer, J. Lohring, J. Luttmann, A. Meissner, J. Weitenberg, M. Traub, T. Sartorius, D. Esser, R. Wester, P. Loosen, and R. Poprawe, IEEE J. Sel. Top. Quantum Electron. **21**, 447 (2015).
20. L. E. Zapata, F. Reichert, M. Hemmer, and F. X. Kärtner, Opt. Lett. **41**, 492 (2016).
21. S. Breitkopf, T. Eidam, A. Klenke, L. von Grafenstein, H. Carstens, S. Holzberger, E. Fill, T. Schreiber, F. Krausz, A. Tunnermann, I. Pupeza, and J. Limpert, Light Sci. Appl. **3**, e211 (2014).
22. J.-P. Negel, A. Loescher, A. Voss, D. Bauer, D. Sutter, A. Killi, M. A. Ahmed, and T. Graf, Opt. Express **23**, 21064 (2015).
23. A. Beyertt, D. Müller, D. Nickel, and A. Giesen, *Advanced Solid-State Photonics* (Optical Society of America, 2004), paper WA5.
24. J. Ahrens, O. Prochnow, T. Binhammer, T. Lang, B. Schulz, M. Frede, and U. Morgner, Opt. Express **24**, 8074 (2016).
25. M. Larionov, F. Butze, D. Nickel, and A. Giesen, Opt. Lett. **32**, 494 (2007).
26. J. Pouysegur, M. Delaigue, Y. Zaouter, C. Hönninger, E. Mottay, A. Jaffrès, P. Loiseau, B. Viana, P. Georges, and F. Druon, Opt. Lett. **38**, 5180 (2013).
27. W. Liu, D. N. Schimpf, T. Eidam, J. Limpert, A. Tünnermann, F. X. Kärtner, and G. Chang, Opt. Lett. **40**, 151 (2015).
28. J. Pouysegur, M. Delaigue, C. Hönninger, Y. Zaouter, P. Georges, F. Druon, and E. Mottay, IEEE J. Sel. Top. Quantum Electron. **21**, 212 (2015).
29. K. Ertel, S. Banerjee, P. D. Mason, P. J. Phillips, M. Siebold, C. Hernandez-Gomez, and J. C. Collier, Opt. Express **19**, 26610 (2011).
30. J. T. Hunt, J. A. Glaze, W. W. Simmons, and P. A. Renard, Appl. Opt. **17**, 2053 (1978).
31. G. H. Kim, J. Yang, A. V. Kulik, E. G. Sall, S. A. Chizhov, V. E. Yashin, and U. Kang, Quantum Electron. **43**, 725 (2013).
32. R. A. Ganeev, I. A. Kulagin, A. I. Ryasnyanskii, R. I. Tugushev, and T. Usmanov, Opt. Spectrosc. **94**, 561 (2003).
33. X. Liu, L. Qian, and F. Wise, Opt. Lett. **24**, 1777 (1999).
34. G. Xie, D. Zhang, L. Qian, H. Zhu, and D. Tang, Opt. Commun. **273**, 207 (2007).
35. S. Hädrich, A. Klenke, A. Hoffmann, T. Eidam, T. Gottschall, J. Rothhardt, J. Limpert, and A. Tünnermann, Opt. Lett. **38**, 3866 (2013).